November 21, 2014

Lattice QCD Study of B-meson Decay Constants from ETMC

A. Bussone [a], N. Carrasco [b], P. Dimopoulos [c,d], R. Frezzotti [c], V. Giménez [e], G. Herdoíza [f], P. Lami [b,g], V. Lubicz [b,g], C. Michael [h], E. Picca [b,g], L. Riggio [b], G.C. Rossi [c,d], F. Sanfilippo [i], A. Shindler [j], S. Simula [b], C. Tarantino [b,g]

ETM Collaboration

[a] *CP^3-Origins & Danish IAS, University of Southern Denmark, Odense M, Denmark*

[b] *INFN, Sezione di Roma Tre, Rome, Italy*

[c] *Dipartimento di Fisica, Università di Roma "Tor Vergata", INFN, Sezione di Tor Vergata, Rome, Italy*

[d] *Museo Storico della Fisica e Centro Studi e Ricerche "Enrico Fermi", Rome, Italy*

[e] *Departament de Física Teòrica and IFIC, Univ. de València-CSIC, València, Spain*

[f] *Instituto de Física Teórica UAM/CSIC and Departamento de Física Teórica, Universidad Autónoma de Madrid, Madrid, Spain*

[g] *Dipartimento di Matematica e Fisica, Università degli Studi Roma Tre, Rome, Italy*

[h] *Theoretical Physics Division, The University of Liverpool, Liverpool, UK*

[i] *School of Physics and Astronomy, University of Southampton, Southampton, UK*

[j] *IAS, IKP, JCHP and JARA-HPC, Forschungszentrum Jülich, Jülich, Germany*

We discuss a lattice QCD computation of the B-meson decay constants by the ETM collaboration where suitable ratios allow to reach the bottom quark sector by combining simulations around the charm-quark mass with an exactly known static limit. The different steps involved in this *ratio method* are discussed together with an account of the assessment of various systematic effects. A comparison of results from simulations with two and four flavour dynamical quarks is presented.

PRESENTED AT

8th International Workshop on the CKM
Unitarity Triangle (CKM 2014)
Vienna, Austria, September 8-12, 2014

1 Introduction

Flavour physics is the place of election where probing the scale of possible extensions of the Standard Model (SM) can be carried out up to energies considerably larger than the ones that can be attained in present-day colliders such as the LHC. A detailed comparison of experimental results to theoretical expectations based solely on the SM is essential to determine its fundamental parameters. The study of the consistency of the determinations of SM parameters by using as many independent processes as possible provides a very stringent test of the theory in its present formulation. For this program to be successful non-perturbative QCD effects contributing to flavour physics processes must be accurately evaluated. In particular lattice QCD studies of hadronic matrix elements of weak operators are essential to test unitarity constraints in the first two rows of the CKM matrix.

Leptonic decays of B-mesons, $B \to \tau\nu$, have been thoroughly studied at the B-factories. A reduction in the relative error on the branching fraction, from $\sim 20\%$ to $\sim 5\%$, is expected to be reached by Belle-II. An improvement in the extraction of the CKM matrix element $|V_{\rm ub}|$ would thus also profit from a more accurate lattice calculation of the B-meson decay constant, f_B. Similarly, rare leptonic decays of neutral B-mesons are being studied by LHC experiments. CMS and LHCb have measured the branching fraction, $\mathcal{B}(B_s \to \mu^+\mu^-)$, with a $\sim 25\%$ relative precision. In this case, the lattice determinations of the B_s-meson decay constant, f_{B_s}, is an important ingredient in the SM prediction of this branching fraction.

The study of the b-quark sector on the lattice requires the development of a dedicated approach. The reason is that the b-quark mass, $m_b \sim 4.2\,\mathrm{GeV}$, is larger than the range of values of the UV cutoff – given by the inverse of the lattice spacing a – that can currently be probed in large-volume lattice QCD simulations, $a^{-1} \lesssim 4\,\mathrm{GeV}$. The condition, $am_b \ll 1$, needed to guarantee the convergence of an expansion in powers of the lattice spacing is therefore not fulfilled. This leads to uncontrolled systematic effects due to lattice artefacts. Several methods, relying to some extent on the use of effective theories, have been developed to address these difficulties (see Ref. [1] for a recent review of the various approaches).

In the following we will discuss the results of the determination of the B-meson decay constants with a method that is based on the construction – directly in QCD – of *ratios* of observables that are well behaved from the point of view of lattice artefacts and that have a precisely known static limit.

2 Approaching the b-quark sector through the ratio method

To illustrate the *ratio method* [2], let us consider an observable, $\Xi(m_h)$, depending on the heavy quark mass m_h according to the scaling laws of heavy quark effective theory (HQET),

$$\Xi(m_h) \;=\; \Xi_{\rm stat} \;+\; \frac{d_1}{m_h} \;+\; \mathrm{O}\left(\frac{1}{m_h^2}\right) , \qquad (1)$$

where $\Xi_{\rm stat}$ refers to the observable in the static limit, $m_h \to \infty$. A well known example is, $\Xi(m_h) = \Phi_{h\ell} = f_{h\ell}\sqrt{M_{h\ell}}$, where $f_{h\ell}$ and $M_{h\ell}$ are the heavy-light ($h\ell$) pseudoscalar meson decay constant and mass, respectively, depending on m_h. By considering a geometric series of quark masses,

$$m_h^{(i+1)} = \lambda\, m_h^{(i)}\,, \qquad i = 1, 2, 3, \ldots \tag{2}$$

with a constant step, $\lambda \gtrsim 1$, and an initial condition, $m_h^{(1)} \approx m_c$, we can construct the following chain equation for Ξ,

$$\Xi(m_b) \;\equiv\; \Xi(m_h^{(K_b)}) \;=\; \Xi(m_h^{(1)}) \;\times\; \frac{\Xi(m_h^{(2)})}{\Xi(m_h^{(1)})} \;\times\; \ldots \;\times\; \frac{\Xi(m_h^{(K_b)})}{\Xi(m_h^{(K_b-1)})}\,, \tag{3}$$

$$\;=\; \Xi(m_h^{(1)}) \;\times\; \prod_{i=2}^{K_b} R(m_h^{(i)})\,, \tag{4}$$

where the ratio $R(m_h^{(i)})$ is defined as follows,

$$R(m_h^{(i)}) \;\equiv\; \frac{\Xi\left(m_h^{(i)}\right)}{\Xi\left(m_h^{(i-1)}\right)}\,. \tag{5}$$

In the example of eq. (4), we have assumed that λ has been tuned in order to reach the b-quark sector after K_b steps. As we will see, this can be achieved by setting $\lambda \approx 1.18$ and $K_b = 10$ but the value of λ and the number of steps K_b can be adapted to the availability of lattice data and to the target accuracy.

On a lattice regularisation of QCD that is improved to remove the lattice artefacts of $\mathrm{O}(a)$, the leading discretisation effects on a quantity $\Xi(m_h)$ involving heavy quarks are of $\mathrm{O}((am_h)^2)$. An advantage of considering the ratio $R(m_h^{(i)})$ in eq. (5) is that those cutoff effects become of order $(\lambda-1)(am_h)^2$ and are therefore significantly suppressed for $\lambda \gtrsim 1$. We stress that the continuum limit can be taken individually for each of the ratios $R(m_h^{(i)})$. The use of ratios allows to control the continuum limit extrapolation up values of m_h that are higher than those attainable by the observable $\Xi(m_h)$ alone. On currently accessible lattice ensembles, we observe that values of $m_h \approx m_b/2$ can be reached, thus significantly reducing the gap towards the b-quark mass.

From eq. (1), one expects that the m_h dependence of the ratios $R(m_h^{(i)})$ follows,

$$R(m_h) \;=\; 1 \;+\; \frac{(\lambda-1)\,\hat{d}_1}{m_h} + \mathrm{O}\left(\frac{1}{m_h^2}\right)\,. \tag{6}$$

The fact that $R(m_h)$ has a precisely known value in the static limit allows to transform the approach to the b-quark sector into an *interpolation* that is constrained by direct determinations up to $m_h \approx m_b/2$. It is also interesting to note that since the $1/m_h$ term in eq. (6) is suppressed by the factor $(\lambda-1) \approx 1/5$, it is in general expected that $1/m_h^2$ can also have a sizeable contribution to the ratios $R(m_h)$.

The implementation of the *ratio method* can be summarised by the following four steps:

(i) Determination of the *triggering point*, $\Xi(m_h^{(1)})$ in the r.h.s of eq. (4), through a direct calculation in the charm quark sector, $m_h^{(1)} \approx m_c$.

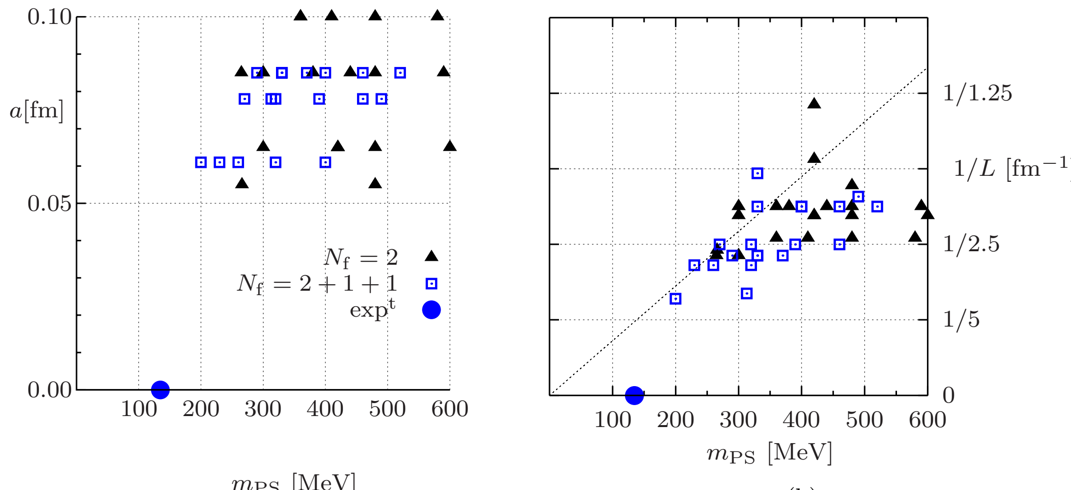

(a) (b)

Figure 1: Range of values of the lattice spacing a, the simulated pion masses M_{PS} and the lattice size L, of ETMC ensembles with $N_{\mathrm{f}} = 2$ and $N_{\mathrm{f}} = 2+1+1$ dynamical quark flavours. The physical pion point is denoted by the blue filled circle. The availability of various values of the lattice spacing is essential for a proper control of the continuum-limit extrapolation in the heavy-quark sector. The oblique line in the right panel denotes, $M_{\mathrm{PS}}L = 3.5$, and the ensembles above this line are used to study finite volume effects.

(ii) Calculation of the ratios $R(m_h^{(i)})$ for a $i = 2, 3, \ldots, \overline{n}$, up to a mass $m_h^{(\overline{n})}$ that permits a proper control of the continuum-limit extrapolation of the ratio.

(iii) The previously computed ratios, $R(m_h^{(i)})$, are used to reach the the b-quark sector through an interpolation using the expected scaling laws of HQET and the fact that the static limit is known, see eq. (6).

(iv) The last step is to apply the chain equation eq. (4) to determine $\Xi(m_b)$.

The fact that the continuum limit is taken at each step of the *ratio method*, implies that it is a regularisation independent approach that can be used with any lattice QCD regularisation. The calculations are performed directly in QCD since the use of HQET only intervenes in guiding the interpolation to the b-quark sector *.

Another attractive aspect of the *ratio method* is that its computational cost is moderate since the computation of quark propagators – for the set of heavy quark masses – can be performed with a multi-mass inverter at the price of a single inversion in the charm sector.

*The knowledge of both the matching to QCD and the running of HQET operators is used to improve this interpolation step. Perturbative or also non-perturbative HQET results can therefore be incorporated in the method. We refer to Ref. [17] for a discussion of the mixing of four-fermion operators.

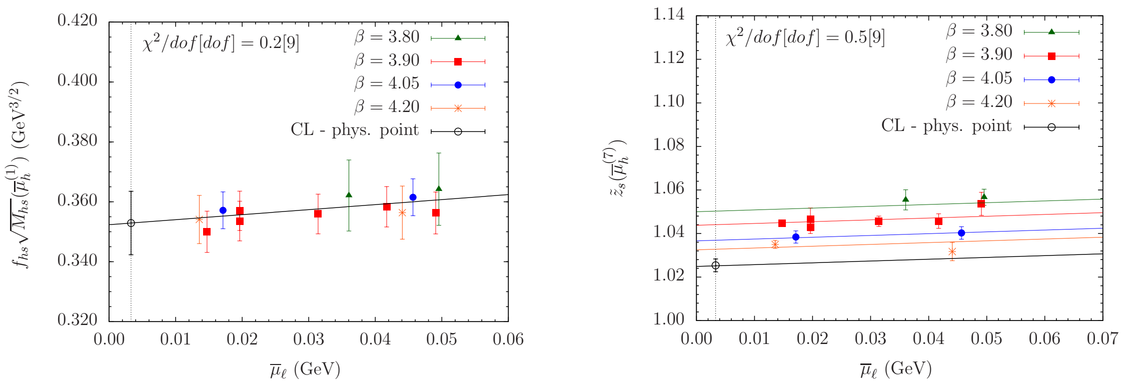

(a) (b)

Figure 2: (a) Results from $N_\mathrm{f} = 2$ dynamical simulations for the light-quark mass dependence of $f_{hs}(\overline{\mu}_h^{(1)})\sqrt{M_{hs}(\overline{\mu}_h^{(1)})}$ at the *triggering point*, corresponding to the charm quark, $\overline{\mu}_h^{(1)} = \overline{\mu}_c$. The good compatibility among measurements at four values of the lattice spacing (denoted by the values of the inverse bare coupling β in the legend) indicates that this observable is not affected by large lattice artefacts. The result in the continuum limit (CL) and at the physical point is shown by the black empty circle [17]. (b) Similarly, we illustrate the case of the heavier quark mass, with $\overline{n} = 7$, for which the ratio $\tilde{z}_s(\overline{\mu}_h^{(7)})$ is computed. We observe that the use of a ratio allows to control the continuum limit extrapolation up to heavy-quark masses, $\overline{\mu}_h^{(7)} \approx 0.6\,\overline{\mu}_b$.

3 Determination of B-meson decay constants

This study is based on lattice QCD simulations performed by the ETM collaboration with $N_\mathrm{f} = 2$ [3,4] and $N_\mathrm{f} = 2+1+1$ [5,6] flavours of Wilson twisted mass fermions at maximal twist [7,8]. Since the quark mass is given by the twisted mass parameter μ, in the following, we will denote the heavy quark mass by, $\overline{\mu}_h = \overline{m}_h$, where the $\overline{\mathrm{MS}}$ scheme at the scale 3 GeV is adopted. The set of available ensembles is illustrated in Fig. 1, where the range of values of the lattice spacing a, the simulated pion masses M_PS and the lattice size L are shown. A first account of simulations at the physical pion mass have been reported in Ref. [9]. ETMC has a dedicated project aiming at precise determinations of observables relevant for flavour physics involving light [10–15] and heavy [2,16–20] quarks.

The decay constant f_{B_s} can be determined via the *ratio method* with various possible choices for the observable $\Xi(\overline{\mu}_h)$. As an illustration we consider, $\Xi(\overline{\mu}_h) = f_{hs}\sqrt{M_{hs}}/C_A^\mathrm{stat}(\overline{\mu}_h)$, but a detailed analysis of how other choices are used assess systematic effects was reported in Ref. [17]. The factor $C_A^\mathrm{stat}(\overline{\mu}_h)$ controls the matching between QCD and HQET and the running of the axial current in the effective theory. With this choice of $\Xi(\overline{\mu}_h)$, the chain equation in eq. (4) can be written as follows,

$$\tilde{z}_s(\overline{\mu}_h^{(2)}) \;\times\; \tilde{z}_s(\overline{\mu}_h^{(3)}) \;\times\; \ldots \;\times\; \tilde{z}_s(\overline{\mu}_h^{(10)}) \;=\; \frac{f_{hs}(\overline{\mu}_h^{(10)})\sqrt{M_{hs}(\overline{\mu}_h^{(10)})}}{f_{hs}(\overline{\mu}_h^{(1)})\sqrt{M_{hs}(\overline{\mu}_h^{(1)})}} \cdot \left[\frac{C_A^\mathrm{stat}(\overline{\mu}_h^{(1)})}{C_A^\mathrm{stat}(\overline{\mu}_h^{(10)})}\right], \quad (7)$$

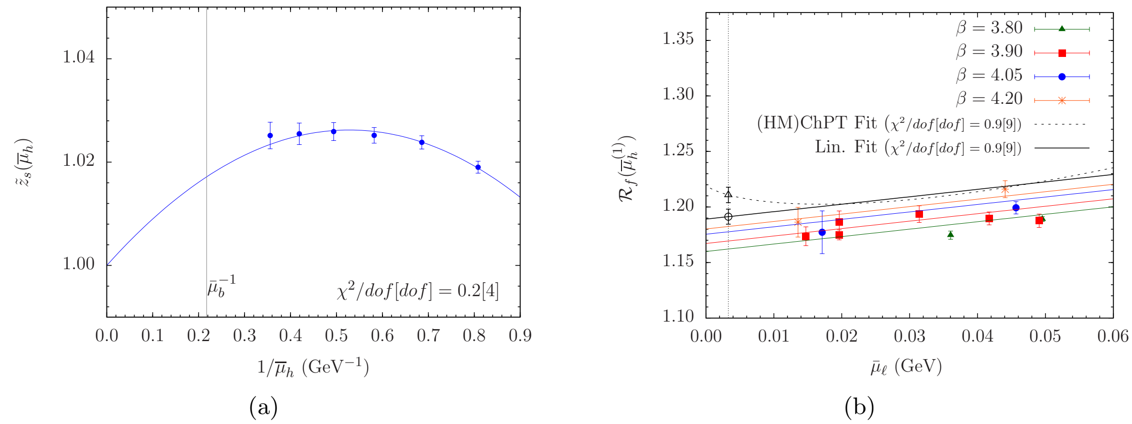

Figure 3: (a) Dependence on the inverse of the heavy quark mass of the ratio $z_s(\overline{\mu}_h)$, in the continuum and for the light-quark physical point, measured in the interval $m_h \in [m_c; 0.6 m_b]$. The blue curve shows a quadratic fit inspired by the HQET expansion which is constrained by the precisely known value in the static limit. The b-quark mass, denoted by the vertical line, is thus reached by an interpolation. A detailed study of the assessment of possible systematic effects was reported in Ref. [17]. (b) Light-quark mass dependence of the double ratio $\mathcal{R}_f$ in eq. (8) – used to determine f_{B_s}/f_B – at the *triggering point*. The deviation between the results of chiral extrapolations based on a linear fit and on a heavy-meson chiral perturbation theory (HMChPT) ansatz is included in the systematic error analysis.

where $\tilde{z}_s(\overline{\mu}_h^{(i)})$ corresponds to the ratio in eq. (5) for the specific choice of $\Xi(\overline{\mu}_h)$. The *triggering point* has been chosen to precisely correspond to the charm quark, $\overline{\mu}_h^{(1)} = \overline{\mu}_c$, and the values, $\lambda = 1.1784$ and $K_b = 10$, have been tuned in order to reach, $\overline{\mu}_h^{(K_b)} = \overline{\mu}_b$, by imposing the physical value of the B-meson mass as an input [17].

The first step of the *ratio method* is illustrated in Fig. 2(a) where the continuum and chiral extrapolations of $f_{hs}\sqrt{M_{hs}}$ at the *triggering point* is shown. The ratios $\tilde{z}_s(\overline{\mu}_h^{(i)})$ are then extracted for $i = 2, 3, \ldots, \overline{n}$. Fig. 2(b) shows that lattice artefacts are under control up to $\overline{n} = 7$, corresponding to the heaviest mass, $\overline{\mu}_h^{(7)} \approx 0.6\,\overline{\mu}_b$. The interpolation of the ratios $\tilde{z}_s(\overline{\mu}_h^{(i)})$ to the b-quark sector is presented in Fig. 3(a). Based on eq. (6), a quadratic fit ansatz inspired by the HQET expansion is constrained to be equal to 1 in the static limit. The last step of the *ratio method* is to use the chain equation in eq. (7) to determine $f_{B_s} \equiv f_{hs}(\overline{\mu}_h^{(10)})$.

The ratio f_{B_s}/f_B can be determined with an observable, $\Xi(\overline{\mu}_h) = \mathcal{R}_f(\overline{\mu}_h)$, defined through a double ratio, in the following way,

$$\mathcal{R}_f(\overline{\mu}_h) = \left[\frac{\left(\frac{f_{hs}(\overline{\mu}_h)}{f_{hl}(\overline{\mu}_h)}\right)}{\left(\frac{f_{sl}}{f_{ll}}\right)} \right] \times \left(\frac{f_K}{f_\pi}\right), \tag{8}$$

where f_K and f_π refer to the physical values of the kaon and pion decay constants, respectively. The chiral extrapolation of $\mathcal{R}_f(\overline{\mu}_h)$ at the *triggering point* is shown in Fig. 3(b). The

source of uncertainty [%]	f_{B_s}	f_{B_s}/f_B	f_B
stat. + fit (C.L. and chiral)	2.2	0.8	2.1
lat. scale	2.0	-	2.0
discr. effects	1.3	0.4	1.7
$1/\mu_h$	1.0	0.1	1.1
chiral extr. trig. point	-	1.7	1.7
total	3.4	2.0	4.0

Table 1: Relative contributions (in percent) to the uncertainties in the determination of f_{B_s}, f_{B_s}/f_B and f_B from our studies with $N_\mathrm{f} = 2$ sea quarks. An overall relative error of 2% is achieved for the dimensionless ratio, f_{B_s}/f_B, while systematic effects coming in particular from scale setting lead to larger relative errors for the individual decay constants. We refer to Ref. [17] for a complete description of the procedures used to determine the statistical and systematic uncertainties.

successive steps of the *ratio method* applied to $\mathcal{R}_f(\overline{\mu}_h)$ are not significantly different than those shown in Figs. 2 and 3(a) and can be found in Ref. [17].

The results for the decay constants in the $N_\mathrm{f} = 2$ case read [17],

$$f_{B_s} = 228(8)\,\mathrm{MeV} \quad , \quad f_B = 189(8)\,\mathrm{MeV} \quad , \quad \frac{f_{B_s}}{f_B} = 1.206(24)\,. \tag{9}$$

The decomposition of the different contributions to the relative error are given in Table 1. Preliminary results from $N_\mathrm{f} = 2+1+1$ simulations [18],

$$f_{B_s} = 235(9)\,\mathrm{MeV} \quad , \quad f_B = 196(9)\,\mathrm{MeV} \quad , \quad \frac{f_{B_s}}{f_B} = 1.201(25)\,, \tag{10}$$

are compatible with the $N_\mathrm{f} = 2$ determinations in eq. (9). This suggests that for these observables, sea-quark effects from strange and charm quarks are smaller than the present accuracy. A comparison of results from various recent lattice QCD determinations is shown in Fig. 4.

4 Conclusions

Physical processes in the quark-flavour sector of the Standard Model can be used to put severe constraints on the parameter space of new physics models. Leptonic decays of B-mesons are a remarkable example of processes that are currently being constrained both from the experimental and the theory side. Lattice QCD calculations of the B-meson decay constants are needed to determine the SM predictions of these decay rates. We have described the results of a method that considers suitable ratios to constrain the approach to the b-quark sector. A comparison of various lattice determinations indicates that f_B and f_{B_s} can currently be determined with a few percent accuracy. No significant effects from strange and charm sea quarks can be observed at this level of precision.

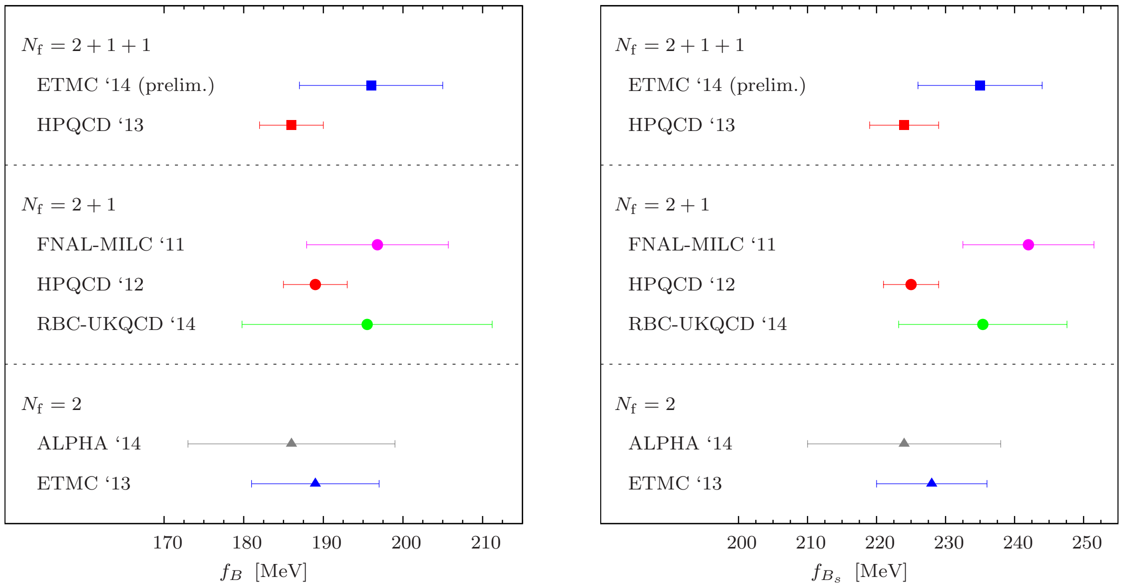

(a) (b)

Figure 4: Comparison of recent lattice QCD determinations [17, 18, 21–25] of the decay constants f_B and f_{B_s} from simulations with $N_f = 2$, $N_f = 2+1$ and $N_f = 2+1+1$ flavours of dynamical quarks. We refer to the recent reviews in Refs. [1, 26–29] for more detailed accounts of these computations.

The *ratio method* has also been used for the determination of other observables in the bottom sector. These include the b-quark mass [2, 16–18], B-mixing bag parameters for the complete basis of four-fermion operators [17] or the form factors of semi-leptonic B-decays [30, 31]. It is interesting to note that preliminary studies with $N_f = 2+1+1$ dynamical quarks indicate that an accuracy $\lesssim 2\%$ can be achieved for the ratio of quark masses, m_b/m_c, via the *ratio method* [20].

ACKNOWLEDGEMENTS

G.H. thanks the organisers for the stimulating environment created during this event. We are grateful to all members of ETMC for fruitful discussions. We acknowledge the CPU time provided by the PRACE Research Infrastructure under the project PRA067 at the Jülich and CINECA SuperComputing Centers, and by the agreement between INFN and CINECA under the specific initiative INFN-lqcd123. We acknowledge computer time made available to us on the Altix system at the HLRN supercomputing service in Berlin under the project "B-physics from lattice QCD simulations". G.H. acknowledges support by the Spanish MINECO through the Ramón y Cajal Programme and through the project FPA2012-31686 and by the Centro de Excelencia Severo Ochoa Program SEV-2012-0249.

References

[1] S. Aoki *et al.* [FLAG], Eur. Phys. J. C **74** (2014) 9, 2890 [arXiv:1310.8555].

[2] B. Blossier *et al.* [ETMC], JHEP **1004** (2010) 049 [arXiv:0909.3187].

[3] P. Boucaud *et al.* [ETMC], Phys. Lett. B **650** (2007) 304 [hep-lat/0701012].

[4] P. Boucaud *et al.* [ETMC], Comput. Phys. Commun. **179** (2008) 695 [arXiv:0803.0224].

[5] R. Baron *et al.* [ETMC], JHEP **1006** (2010) 111 [arXiv:1004.5284].

[6] R. Baron *et al.* [ETMC], Comput. Phys. Commun. **182** (2011) 299 [arXiv:1005.2042].

[7] R. Frezzotti *et al.* [ALPHA], JHEP **0108** (2001) 058 [hep-lat/0101001].

[8] R. Frezzotti and G. C. Rossi, JHEP **0408** (2004) 007 [hep-lat/0306014].

[9] A. Abdel-Rehim *et al.* [ETMC], PoS LATTICE **2013** (2013) 264 [arXiv:1311.4522].

[10] B. Blossier *et al.* [ETMC], JHEP **0804** (2008) 020 [arXiv:0709.4574].

[11] B. Blossier *et al.* [ETMC], JHEP **0907** (2009) 043 [arXiv:0904.0954].

[12] R. Baron *et al.* [ETMC], JHEP **1008** (2010) 097 [arXiv:0911.5061].

[13] B. Blossier *et al.* [ETMC], Phys. Rev. D **82** (2010) 114513 [arXiv:1010.3659].

[14] F. Farchioni *et al.* [ETMC], PoS LATTICE **2010** (2010) 128 [arXiv:1012.0200].

[15] R. Baron *et al.* [ETMC], PoS LATTICE **2010** (2010) 123 [arXiv:1101.0518].

[16] P. Dimopoulos *et al.* [ETMC], JHEP **1201** (2012) 046 [arXiv:1107.1441].

[17] N. Carrasco *et al.* [ETMC], JHEP **1403** (2014) 016 [arXiv:1308.1851].

[18] N. Carrasco *et al.* [ETMC], [arXiv:1311.2837].

[19] N. Carrasco *et al.* [ETMC], Nucl. Phys. B **887** (2014) 19 [arXiv:1403.4504].

[20] A. Bussone *et al.* [ETMC], [arXiv:1411.0484].

[21] R. J. Dowdall *et al.* [HPQCD], Phys. Rev. Lett. **110** (2013) 22, 222003 [arXiv:1302.2644].

[22] A. Bazavov *et al.* [Fermilab-MILC], Phys. Rev. D **85** (2012) 114506 [arXiv:1112.3051].

[23] H. Na *et al.* [HPQCD], Phys. Rev. D **86** (2012) 034506 [arXiv:1202.4914].

[24] N. H. Christ *et al.* [RBC-UKQCD], [arXiv:1404.4670].

[25] F. Bernardoni *et al.* [ALPHA], Phys. Lett. B **735** (2014) 349 [arXiv:1404.3590].

[26] C. Bouchard, talk at the lattice conference (2014).

[27] A. El-Khadra, talk at this conference (2014).

[28] W. Lucha, D. Melikhov and S. Simula, [arXiv:1411.3890].

[29] N. Tantalo, talk at this conference (2014).

[30] M. Atoui *et al.* Eur. Phys. J. C **74** (2014) 2861 [arXiv:1310.5238].

[31] F. Sanfilippo, talk at this conference (2014).